



Signatures of coherent propagation of blue polaritons in Cu₂O

Johannes Schmutzler, Dietmar Fröhlich, and Manfred Bayer

Experimentelle Physik 2, Technische Universität Dortmund, D-44221 Dortmund, Germany

(Received 24 October 2012; revised manuscript received 15 January 2013; published 4 June 2013)

Double resonant sum-frequency generation (SFG) is demonstrated in Cu₂O. The 1S yellow orthoexciton-polariton is resonantly excited by a single frequency dye laser (quadrupole transition) and coupled to the blue 1S exciton-polariton by a single frequency infrared laser (dipole transition). Sum-frequency (SF) spectra as a function of the energy of the infrared laser are measured for the two pump laser beams parallel and antiparallel. In the antiparallel configuration, pronounced oscillations are observed with a period scaling inversely with the crystal length. The origin of these oscillations is discussed in detail and attributed to a phase-matching effect. The appearance of phase matching can be understood if the blue polaritons—generated by SFG—move coherently through the crystal. This observation is very surprising, since blue exciton-polaritons excited in a one-photon transmission experiment exhibit an absorption length of only 100 nm due to strong scattering.

DOI: [10.1103/PhysRevB.87.245202](https://doi.org/10.1103/PhysRevB.87.245202)

PACS number(s): 78.20.-e, 71.36.+c

I. INTRODUCTION

Nonlinear spectroscopy of solids¹ is a mature field leading to information on electronic properties not accessible by linear optical methods. Considering only two-photon processes, there are additional degrees of freedom available, since polarization vectors \vec{e}_i and wave vectors \vec{k}_i ($i = 1, 2$) of both photon beams can be set separately, allowing k -space spectroscopy.^{1,2} Besides spectroscopic data, nonlinear observations linked to coherent propagation of the excitation can be investigated. A text-book example are the so-called Maker fringes observed in second-harmonic generation.³⁻⁵ Another example is the coherent propagation of polaritons, which is observed as a beatlike structure in time-resolved experiments.⁶

So far, light generated by sum-frequency generation (SFG) could be extracted out of a nonlinear material with high efficiency only for energies below or close to the band gap, otherwise strong absorption occurs. Further, nonlinear effects have required power levels in the kilowatt to megawatt range, necessitating pulsed laser sources. By spectrally narrow excitation of two exciton-polariton resonances in Cu₂O, we achieve strong SF signals far above the band gap with continuous wave lasers in the milliwatt to watt power range.

The lowest excitons of the so-called yellow series in Cu₂O are intensively studied because they are considered as candidates for Bose-Einstein condensation (BEC) in a three-dimensional system.⁷⁻¹⁰ Excitation from the upmost valence band of Γ_7^+ symmetry to the lowest conduction band of Γ_6^+ symmetry leads to orthoexcitons (Γ_5^+ symmetry) and paraexcitons (Γ_2^+ symmetry), which are optically forbidden and split off by 12 meV to lower energy from the quadrupole allowed orthoexcitons.

Besides the yellow exciton series, there are three other series, the states of which are named green, blue, and violet excitons according to their spectral range of absorption. The green series is due to excitation from a Γ_8^+ -valence band (split off by 130 meV from the Γ_7^+ -valence band of the yellow series) to the same Γ_6^+ -conduction band. The blue and violet excitons stem from the same Γ_7^+ - and Γ_8^+ -valence bands, respectively, and an odd parity conduction band of Γ_8^- symmetry (see the inset of Fig. 1). The S excitons of these series are dipole allowed. In contrast to the yellow and green

series, there are not many experiments reported on the blue and violet series. Reflectivity and transmission measurements of very thin films ($\propto 100$ nm) were reported in the 1960's.¹¹⁻¹³ Later, the optical properties were studied by spectroscopic ellipsometry.¹⁴ Because of the large oscillator strength of the blue and violet excitons, one expects a pronounced polariton structure, which was not investigated up to now.

In this contribution, we present a nonlinear spectroscopic approach of investigating 1S-blue polaritons in natural Cu₂O crystals of several 10- μ m thickness. With the use of two narrow band cw lasers (dye and infrared lasers), we are able to excite blue polaritons by SFG. A sum-frequency (SF) signal is only seen if the dye laser is tuned to the resonance of the yellow 1S orthoexciton. It was shown before that 1S yellow orthoexciton-polaritons propagate coherently through rather thick samples ($\propto 1$ mm)⁶ with group velocities as low as 40 km/s¹⁵ whereas the off-resonant polaritons in the infrared spectral range exhibit a group velocity of about 100 000 km/s. Thus our experiment provides the unique opportunity to investigate the interaction of polaritons with a group velocity difference of three orders of magnitude. A possible consequence of this experimental situation is the observation of coherent propagation in a spectral range of high absorption: it is expected that because of the large damping of blue polaritons with energies 0.5 eV above the band gap (absorption length ≈ 100 nm),¹¹ the SF emission originates only from the last 100 nm of the crystal. Nevertheless, we observe in the antiparallel configuration a pronounced beatlike structure which can be understood if one assumes coherent propagation of blue polaritons through the rather thick crystal (about 600 times the absorption length).

In Sec. II, we derive the selection rules for SFG and the polariton dispersion for the blue and violet excitons. The experimental setup is described in Sec. III followed by a presentation of our experimental results in Sec. IV. Finally, we present in Sec. V our conclusions with an outlook on further experiments.

II. THEORY

Despite the fact that Cu₂O is a semiconductor with inversion symmetry, SFG is observed, showing characteristic dependencies on crystal orientation and polarization. We consider

a three-step process. In a first step, the 1S orthoexciton of the yellow series (Γ_5^+ symmetry) is excited by a quadrupole transition (even parity operator Γ_5^+), in a second step, the Γ_5^+ orthoexciton is coupled to the 1S orthoexciton of the blue series (Γ_4^- symmetry) by a dipole transition (odd parity operator Γ_4^-). Finally, in a third step, a photon is emitted by a dipole transition to the ground state.

Using the coupling coefficients of the Tables of Koster *et al.*¹⁶ for the above three steps, one can easily derive detailed polarization selection rules for all crystal orientations. For the first step, the amplitude QA for the quadrupole transition to the Γ_5^+ orthoexciton is given by the symmetric vector product

$$QA = \vec{e}_{\text{dye}} \otimes \vec{k}_{\text{dye}}, \quad (1)$$

where \vec{e}_{dye} and \vec{k}_{dye} refer to the polarization and k vector of the dye laser, respectively. Coupling in the second step the Γ_5^+ orthoexciton to the blue Γ_4^- orthoexciton [the electron in the Γ_6^+ -conduction band is lifted by the infrared laser into the Γ_8^- -conduction band (Fig. 1 inset)] leads to the amplitude SFA of the Γ_4^- state:

$$\text{SFA} = [\vec{e}_{\text{dye}} \otimes \vec{k}_{\text{dye}}] \otimes \vec{e}_{\text{ir}}, \quad (2)$$

where \vec{e}_{ir} refers to the polarization of the infrared laser. Finally, one has to decompose this vector into its transverse and longitudinal components with respect to the wave vector \vec{k}_{dye} . Only the transverse components lead to SFG [transversal polaritons (TPs) in Fig. 1]. As shown in Table I, one can also excite longitudinal excitons (LEs, polarization parallel $\vec{k}_{\text{dye}} = [111]$). According to the selection rules derived [Eq. (2)], there is no SFG expected for $\vec{k}_{\text{dye}} = [100]$ and $[110]$. Therefore we have used crystals oriented for $\vec{k}_{\text{dye}} = [111]$.

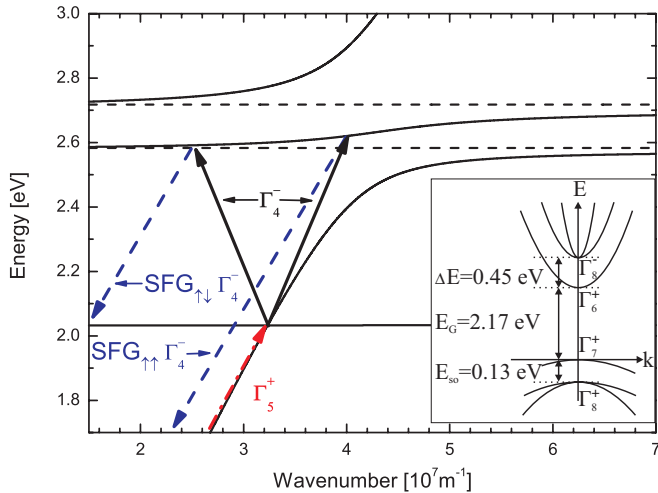


FIG. 1. (Color online) Polariton diagram of a three-oscillator model. Three-step process of the experimental approach is indicated by arrows. Black solid line, TP dispersion according to Eq. (3); dashed horizontal lines, resonances of blue and violet LEs; red dash-dotted arrow, quadrupole excitation (Γ_5^+ symmetry) of 1S yellow orthoexciton; black arrows, dipole transition (Γ_4^- symmetry) to the middle polariton branch from 1S yellow orthoexciton for parallel/antiparallel beam propagation; blue dashed arrows, SFG (Γ_4^- symmetry) for parallel/antiparallel beam propagation. (Inset) Schematic band structure of Cu_2O close to the Γ point.

TABLE I. Relative oscillator strength for different polarizer and analyzer configurations and $\vec{k}_{\text{dye}} = [111]$. f_{tp} (f_{le}) denote the relative oscillator strength for TP (LE).

\vec{e}_{dye}	\vec{e}_{ir}	Analyzer	f_{tp}	f_{le}
$\bar{1}\bar{1}0$	$\bar{1}\bar{1}0$	$\bar{1}\bar{1}0$	0	1/9
$\bar{1}\bar{1}0$	$\bar{1}\bar{1}0$	$\bar{1}\bar{1}\bar{2}$	2/9	1/9
$\bar{1}\bar{1}0$	$\bar{1}\bar{1}\bar{2}$	$\bar{1}\bar{1}0$	2/9	0
$\bar{1}\bar{1}0$	$\bar{1}\bar{1}\bar{2}$	$\bar{1}\bar{1}\bar{2}$	0	0
$\bar{1}\bar{1}\bar{2}$	$\bar{1}\bar{1}0$	$\bar{1}\bar{1}0$	2/9	0
$\bar{1}\bar{1}\bar{2}$	$\bar{1}\bar{1}0$	$\bar{1}\bar{1}\bar{2}$	0	0
$\bar{1}\bar{1}\bar{2}$	$\bar{1}\bar{1}\bar{2}$	$\bar{1}\bar{1}0$	0	1/9
$\bar{1}\bar{1}\bar{2}$	$\bar{1}\bar{1}\bar{2}$	$\bar{1}\bar{1}\bar{2}$	2/9	1/9

In order to elucidate the kinematics of the SFG processes, we model the polariton dispersion taking into account three resonances. The inclusion of the violet exciton resonance [0.13 eV above the blue exciton resonance (inset of Fig. 1)] is of great importance, since the upper polariton branch of the blue exciton resonance is strongly influenced (pushed down) by the violet polariton. We therefore diagonalize the 4×4 matrix,¹⁷ which couples the photon dispersion $E_{\text{ph}}(k)$ with the three exciton resonances $E_y(k)$ (yellow 1S orthoexciton), $E_b(k)$ (blue 1S exciton), and $E_v(k)$ (violet 1S exciton):

$$H = \begin{pmatrix} E_{\text{ph}}(k) & \frac{\sqrt{f_y}E_{y,0}}{2} & \frac{\sqrt{f_b}E_{b,0}}{2} & \frac{\sqrt{f_v}E_{v,0}}{2} \\ \frac{\sqrt{f_y}E_{y,0}}{2} & E_y(k) & 0 & 0 \\ \frac{\sqrt{f_b}E_{b,0}}{2} & 0 & E_b(k) & 0 \\ \frac{\sqrt{f_v}E_{v,0}}{2} & 0 & 0 & E_v(k) \end{pmatrix}. \quad (3)$$

For the yellow 1S orthoexciton, $f_y = 1.3 \times 10^{-9}$ and $E_{y,0} = 2.032775$ eV are taken from Ref. 18 (note that for $k = [111]$ the oscillator strength is reduced by a factor 3 as compared to $k = [001]$). $f_b = 1.2 \times 10^{-2}$, $f_v = 2.1 \times 10^{-2}$, $E_{b,0} = 2.576$ eV, and $E_{v,0} = 2.703$ eV denote the oscillator strengths and resonance energies of the blue and the violet excitons taken from Ref. 11, respectively. Spatial dispersion is taken into account, using the same mass $m = 3m_0$ (m_0 corresponds to the free electron mass).¹⁹ $E_y(k) = E_{y,0} + \frac{\hbar^2 k^2}{2m}$, $E_b(k) = E_{b,0} + \frac{\hbar^2 k^2}{2m}$, and $E_v(k) = E_{v,0} + \frac{\hbar^2 k^2}{2m}$. $\sqrt{f_y}E_{y,0}$, $\sqrt{f_b}E_{b,0}$, and $\sqrt{f_v}E_{v,0}$ denote the corresponding Rabi energies. The photon dispersion is given by $E_{\text{ph}}(k) = \hbar ck/n_b$, where $n_b = 3$ is assumed for the background refractive index in the visible spectral range.

In Fig. 1, the polariton diagram for the three oscillator model is shown. The kinematics of our experimental setup lead to resonances on the middle polariton branch. As outlined above, the 1S orthoexciton-polariton is pumped by the dye laser. Depending on the direction of the infrared laser (parallel or antiparallel to the dye laser), two different resonances on the middle polariton branch are excited, which lead to two different SF signals.

III. EXPERIMENTAL SETUP

The high-resolution setup is shown schematically in Fig. 2. In the first step of SFG, we use a single-frequency dye laser

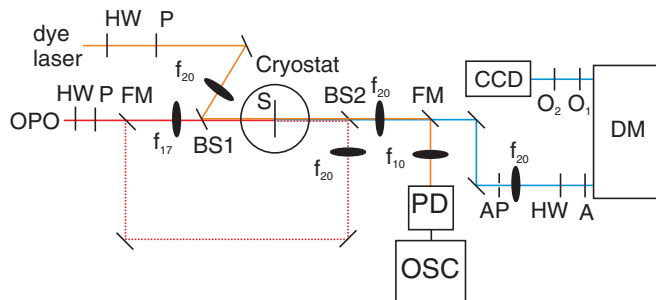


FIG. 2. (Color online) Schematic setup for SFG spectroscopy: A, analyzer; AP, aperture; BS1, silicon beam splitter; BS2, beam splitter; CCD, charge coupled device camera; DM, double monochromator; f_{xx} , lens with xx -cm focal length; FM, flip mirror; HW, half-wave plate; O_1 and O_2 , photo-objectives; OPO, optical-parametric oscillator; OSC, oscilloscope; P, polarizer; PD, photo diode; S, sample.

with linewidth <5 neV and power <100 mW (Coherent 899-29) for resonant excitation of the yellow 1S orthoexciton-polariton. For the excitation of the blue exciton-polariton, we use in the second step a single-frequency optical-parametric-oscillator (OPO, Aculight Argos 2400 CW OPO, linewidth <5 neV, power <1 W). The OPO covers an energy range of 0.496–0.568 eV and 0.602–0.683 eV for idler and signal outputs, respectively. Due to the degeneracy point of the OPO at 0.583 eV, there is a gap in the tuning range between 0.568–0.602 eV. The polarization of dye laser and OPO can be set by half-wave plates and polarizers. The dye beam is focused via a silicon beam splitter (transparent for the IR beam from the OPO) on the sample. For focusing the infrared beam, we use a BaF₂ lens. With a flip mirror and an additional beam splitter, we can switch between the parallel and antiparallel configuration. For the adjustment of overlap of the laser beams, a 100- μ m pinhole is mounted on the sample holder. Measurements were performed at 1.5 K using a He-bath cryostat. The SF signal in the blue spectral region is measured with a nitrogen-cooled CCD camera behind a double monochromator (second order). The polarization anisotropy of the monochromator was taken into account by setting the analyzer to the preferred polarization of the monochromator. The polarization of the SF signal is then measured by tuning the half-wave plate. Two high-quality photo-objectives provide a magnification by factor 4 on the CCD. The observed linewidth of the SF is limited by the resolution of our monochromator to 10 μ eV. For tuning the dye laser into resonance, we use a photodiode and an oscilloscope. As discussed in detail in Ref. 20, strain-free mounting of the sample is very important. Nevertheless, it was still necessary to select the right spot on the sample in order to achieve a narrow resonance of about 2.5 μ eV as seen in Fig. 3. The samples (thickness 30 and 60 μ m) are cut from a high-quality natural crystal and oriented along [111] (because of selection rules, as derived in Sec. II).

IV. RESULTS AND DISCUSSION

In this section, we will first show that we are dealing with resonant SFG as outlined in Sec. II. We will present a power

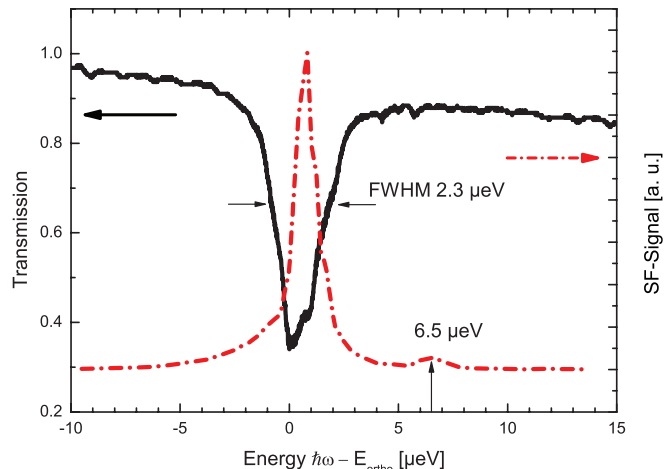


FIG. 3. (Color online) Black line, absorption spectrum of yellow 1S orthoexciton; red dash-dotted line, excitation spectrum of SF signal as a function of dye laser-energy for fixed setting of OPO. Maximum of absorption is at $E_{\text{ortho}} = 2.032788$ eV.

and a polarization dependence that confirms the selection rules (see Table I). We will then show the SF spectra for the parallel and antiparallel beam configurations. The most striking result is the occurrence of a pronounced beatlike structure in the spectra of the antiparallel configuration, which gives evidence for a coherent propagation of blue polaritons. Here, the propagation length in our SFG experiments is at least a factor 600 larger than the absorption length of about 100 nm, as known from one-photon experiments.¹¹

The resonance dependence of the blue SF signal is shown in Fig. 3. The narrow excitation spectrum clearly proves that a narrow band laser is a prerequisite for observing SFG in this study. The additional small resonance at about 6.5 μ eV is explained by a fine structure due to wave-vector-dependent exchange interaction as reported in Ref. 20.

In Fig. 4, the power dependence is presented. As expected, the SF signal depends linearly on the product of the power levels of both lasers. By placing an iris in the telescopic setup, it was confirmed that the SF beam is collinear to the pump beams. The inset of Fig. 4 shows a typical SF signal. The full width at half maximum is about 10 μ eV, which is limited by the spectral resolution of the monochromator.

In the inset of Fig. 5, we show a detailed polarization dependence of the SF signal for the incoming polarizations $\vec{e}_{\text{dye}} = [11\bar{2}]$ and $\vec{e}_{\text{ir}} = [1\bar{1}0]$. As seen from Table I, the SF signal vanishes for the analyzer in $[11\bar{2}]$ and exhibits a maximum for $[1\bar{1}0]$. The other polarization dependencies according to Table I are also confirmed. We performed measurements of crystals oriented along $\vec{k}_{\text{dye}} = [100]$ and $[110]$. As expected from Eq. (2), no SFG was observed.

In Figs. 5(a)–5(c), we present the SF spectra for the parallel and antiparallel beam configurations, respectively. In the parallel beam configuration [see Fig. 5(a)], we find a resonance centered at about 2.595 eV with a FWHM of 10 meV, which is attributed to phase matching (energy and momentum conservation) on the middle polariton branch as shown in Fig. 1.

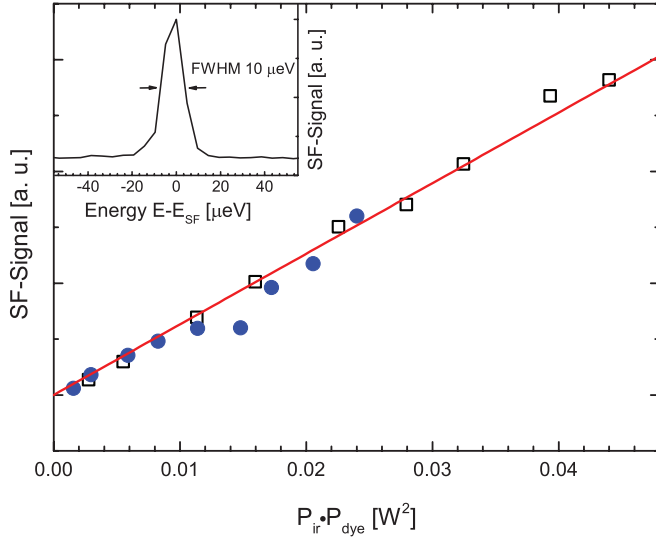


FIG. 4. (Color online) Dependence of SF-signal on product of dye laser (P_{dye}) and OPO power (P_{ir}). Blue closed circles, $P_{\text{dye}} = 30$ mW; black open squares, $P_{\text{dye}} = 55$ mW; red line, linear fit. (Inset) Typical SF spectrum.

In the antiparallel configuration [see Figs. 5(b) and 5(c)], however, oscillations of the SF signal are clearly seen. At first sight, the most obvious interpretation of these oscillations seems to be the occurrence of a standing wave of the OPO beam in the sample. One expects from the large absorption coefficient in the blue spectral range that the emission of SF stems only from the last 100 nm. In the case of a node at the sample boundaries, one would expect a decrease of the SF signal. However, using the Fresnel formula, one can deduce an reflection coefficient of $R = \frac{(n_{\text{ir}}-1)^2}{(n_{\text{ir}}+1)^2} \approx 20\%$, where $n_{\text{ir}} = 2.55$ is the refractive index in the infrared spectral range as reported in Ref. 21. This corresponds to a finesse of $F = \frac{4R}{(1-R)^2} \approx 0.8$ and a minimal transmission at the nodes of $T_{\text{min}} = \frac{1}{1+F} \approx 0.55$. Since we show in Fig. 4 that the intensity of the SF-signal scales linearly with the OPO laser power one would expect only a suppression by a factor of 2 and not by a factor of up to 50 as shown in our data [see Figs. 5(b) and 5(c)]. Besides, standing waves should also be observable in the parallel beam configuration.

An alternative explanation for the occurrence of these oscillations is a phase-matching effect. As discussed in Ref. 4, these so-called Maker fringes should be quenched if the nonlinear medium is absorbing. In our case, the absorption length is even almost three orders of magnitude smaller than the thickness of the crystal.¹¹⁻¹³ Thus the occurrence of oscillations, which are related to a phase matching effect, can only be explained, if one assumes a coherent propagation of the blue polaritons through the crystal. The condition for phase matching $\Delta k = 0$ is fulfilled on the middle polariton branch, where the polariton slopes of the OPO-beam starting from the 1S yellow orthoexciton-polariton resonance (see Fig. 1) intersect. The SF signal I_{SF} for a transparent medium is given by⁴

$$I_{\text{SF}} \propto \frac{[\sin(\Delta k L/2)]^2}{(\Delta k L/2)^2}, \quad (4)$$

where L denotes the length of the crystal.

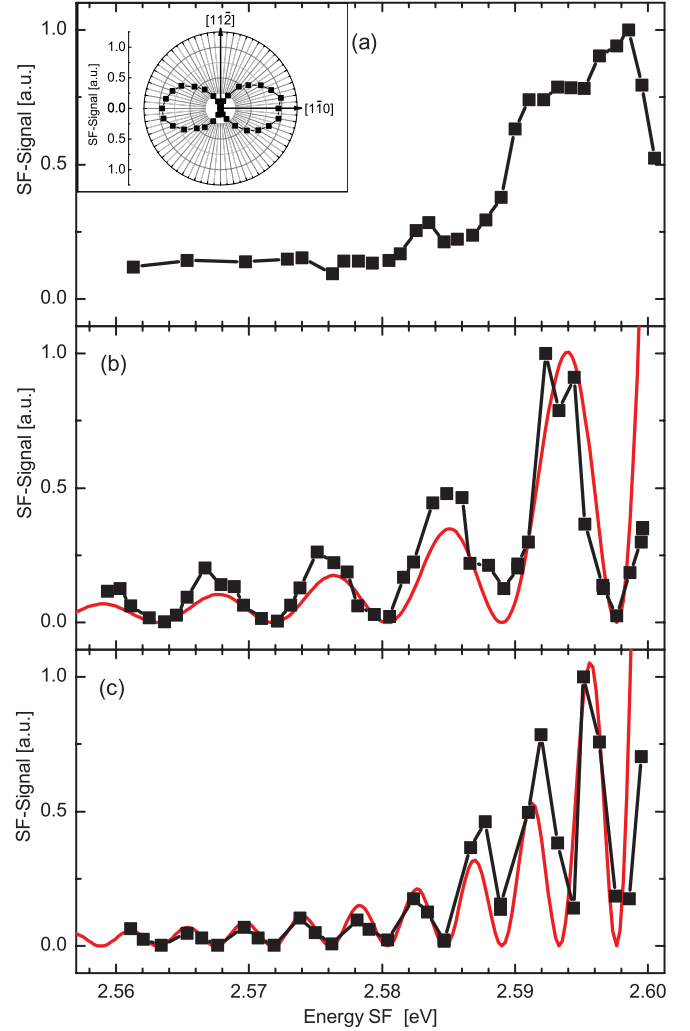


FIG. 5. (Color online) (a) Blue exciton-polariton resonance in the parallel beam configuration for the $30 \mu\text{m}$ sample. (b) and (c) Blue exciton-polariton resonance in the antiparallel beam configuration for the $30 \mu\text{m}$ and the $60 \mu\text{m}$ sample. Black squares, data; red line, calculated curve according to Eqs. (4) and (5). (Inset) Polarization dependence of SF-signal with respect to the crystal axis $[11\bar{2}]$ and $[\bar{1}10]$ ($\vec{k}_{\text{dye}} = [111]$). Incoming polarizations are $\vec{e}_{\text{dye}} = [11\bar{2}]$ and $\vec{e}_{\text{ir}} = [\bar{1}10]$. Signal intensity is proportional to the radial distance from the center.

For parallel (antiparallel) configuration the phase mismatch Δk is given by

$$\Delta k = 2\pi \left[\frac{n_{\text{sf}\uparrow\uparrow(\uparrow\downarrow)}}{\lambda_{\text{SF}}} - \frac{n_{\text{ortho}}}{\lambda_{\text{ortho}}} (\mp) \frac{n_{\text{ir}}}{\lambda_{\text{ir}}} \right], \quad (5)$$

where $n_{\text{sf}\uparrow\uparrow(\uparrow\downarrow)}$ is the refractive index for the SF polariton in the parallel (antiparallel) configuration, n_{ortho} for the yellow 1S orthoexciton and n_{ir} for the infrared spectral range. λ_{SF} , λ_{ortho} , and λ_{ir} are the corresponding wavelengths in vacuum.

A more rigorous treatment would have to include damping processes in the polariton analysis. This might also explain that for the overall fit of the phase-match analysis a rather high refractive index of the resonantly excited 1S orthoexciton-polariton ($n_{\text{ortho}} = 3.6$) was derived as compared to the previously reported background refractive index $n_{\text{ortho}} = 2.95$.²²

With $n_{\text{ir}} = 2.55$ in the infrared spectral range and phase matching $\Delta k = 0$ at an energy of 2.6062 eV, we can fit the experimental data for the antiparallel beam configuration well for the 30- and the 60- μm thick samples [see Figs. 5(b) and 5(c)]. Unfortunately, the spectral range between 2.600–2.630 eV is not accessible to our OPO system due to the before mentioned gap in the tuning range, we could therefore not study the phase matching condition directly. The fact, that no oscillations for the parallel configuration are observed, can be deduced from Eqs. (4) and (5). The corresponding phase matching spectrum is oscillating with a large period of about 50 meV, the resonance is thus not influenced by the phase matching effect.

If there would be an appreciable absorption of the coherently excited blue excitons due to relaxation processes to lower excitons (e.g., dipole-allowed P-excitons of yellow series), one would expect an emission shifted to lower energy from the observed SF emission. We have carefully scanned the spectral region down to the yellow series without observing any emission.

V. CONCLUSION AND OUTLOOK

In conclusion, we have achieved efficient SFG in Cu_2O , a crystal with inversion symmetry, using two continuous wave lasers of rather low power (<100 mW, <1 W). The selection rules for a quadrupole-dipole SFG process are confirmed in detail. The most surprising observation is the occurrence of pronounced oscillations, which are observed *only* in the antiparallel configuration. We discuss in detail the origin of this effect and present evidence for a coherent propagation of blue polaritons in crystals up to 600 times thicker than the absorption length, which is known from transmission measurements.^{11–13} The reason for this unexpected observation might be the rather unique situation of our experimental approach. Firstly, we use two single frequency laser systems. Consequently, we excite polaritons with very well defined energies and wave vectors. Therefore intercarrier scattering is expected to be significantly reduced due to a

lack of available scattering channels that fulfill energy and momentum conservation according to Fermi's "golden rule". Secondly, two coherently propagating polariton beams with a difference in group velocity by three orders of magnitude fuse to generate a SF polariton beam. We have discussed in detail a possible alternative interpretation of our results in terms of simple interference effects, which also lead to a thickness dependent pattern. This pattern would be expected for both configurations contrary to our findings. The missing beatlike pattern in the parallel configuration, however, is explained by our analysis assuming Maker-fringes. In addition, the large ratio of contrast (up to factor of 50) as compared to a factor of 2 expected in an interference pattern, is a good argument for our interpretation. Unfortunately for experimental reasons, we cannot scan into the resonance of the Maker fringes. As mentioned before, a weak point in our polariton analysis lies in the fact that we neglected damping. As a concept for a theoretical treatment of SFG it might be advantageous to start with polariton eigenstates as basis states and interpret SFG as a fusion of two incoming polaritons into an outgoing polariton as was first proposed in Ref. 23. Due to the large difference in group velocity of the participating polariton beams in our experiments, the polariton fusion concept is of even more relevance than in experiments discussed so far.^{24–26} For the resonantly excited 1S orthoexciton, a group velocity down to 40 km/s was measured,¹⁵ whereas for the nonresonantly excited infrared polaritons the group velocity is about 100 000 km/s. Thus a rigorous theoretical treatment of our experimental results in terms of Bloch equations using polaritons as basis states could elucidate the origin of the observed beats.

For future experiments, it might be promising to look for an *interband* dynamic Stark effect using an infrared laser of higher power. An *intraband* dynamic Stark effect of yellow excitons has already been reported in Ref. 27.

ACKNOWLEDGMENT

We acknowledge the support by the Deutsche Forschungsgemeinschaft (BA 1549/18-1).

¹*Nonlinear Spectroscopy of Solids: Advances and Applications*, edited by B. Di Bartolo (Plenum Press, New York, 1994).

²D. Fröhlich, E. Mohler, and P. Wiesner, *Phys. Rev. Lett.* **26**, 554 (1971).

³P. D. Maker, R. W. Terhune, M. Nisenoff, and C. M. Savage, *Phys. Rev. Lett.* **8**, 21 (1962).

⁴Y. R. Shen, *The Principles of Nonlinear Optics* (John Wiley & Sons, New York, 1984).

⁵R. W. Boyd, *Nonlinear Optics* (Academic Press, San Diego, 1992).

⁶D. Fröhlich, A. Kulik, B. Uebbing, A. Mysyrowicz, V. Langer, H. Stolz, and W. von der Osten, *Phys. Rev. Lett.* **67**, 2343 (1991).

⁷S. Denev and D. W. Snoke, *Phys. Rev. B* **65**, 085211 (2002).

⁸C. Sandfort, J. Brandt, C. Finke, D. Fröhlich, M. Bayer, H. Stolz, and N. Naka, *Phys. Rev. B* **84**, 165215 (2011).

⁹R. Schwartz, N. Naka, F. Kieseling, and H. Stolz, *New J. Phys.* **14**, 023054 (2012).

¹⁰K. Yoshioka, E. Chae, and M. Kuwata-Gonokami, *Nat. Commun.* **2**, 328 (2011).

¹¹A. Daunois, J. L. Deiss, and B. Meyer, *J. Phys. France* **27**, 142 (1966).

¹²S. Brahms and S. Nikitine, *Solid State Commun.* **3**, 209 (1965).

¹³S. Brahms, S. Nikitine, and J. Dahl, *Phys. Lett.* **22**, 31 (1966).

¹⁴T. Ito, T. Kawashima, H. Yamaguchi, T. Masumi, and S. Adachi, *J. Phys. Soc. Jpn.* **67**, 2125 (1998).

¹⁵D. Fröhlich, G. Dasbach, G. B. H. von Högersthal, M. Bayer, R. Klieber, D. Suter, and H. Stolz, *Solid State Commun.* **134**, 139 (2005).

¹⁶G. F. Koster, J. O. Dimmock, R. G. Wheeler, and H. Statz, *Properties of the Thirty-Two Point Groups* (M.I.T. Press, Cambridge, Massachusetts, 1963).

¹⁷T. Baars, G. Dasbach, M. Bayer, and A. Forchel, *Phys. Rev. B* **63**, 165311 (2001).

- ¹⁸D. Fröhlich, J. Brandt, C. Sandfort, M. Bayer, and H. Stolz, *Phys. Status Solidi B* **243**, 2367 (2006).
- ¹⁹D. Fröhlich, J. Brandt, C. Sandfort, M. Bayer, and H. Stolz, *Phys. Rev. B* **84**, 193205 (2011).
- ²⁰G. Dasbach, D. Fröhlich, R. Klieber, D. Suter, M. Bayer, and H. Stolz, *Phys. Rev. B* **70**, 045206 (2004).
- ²¹M. O'Keefe, *J. Chem. Phys.* **39**, 1789 (1963).
- ²²J. Brandt, D. Fröhlich, C. Sandfort, M. Bayer, H. Stolz, and N. Naka, *Phys. Rev. Lett.* **99**, 217403 (2007).
- ²³L. N. Ovander, *Sov. Phys. Usp.* **8**, 337 (1965).
- ²⁴D. Fröhlich, E. Mohler, and C. Uihlein, *Phys. Status Solidi B* **55**, 175 (1973).
- ²⁵*Polaritons*, edited by E. Burstein and F. De Martini (Pergamon Press, New York, 1974), p. 303.
- ²⁶R. Girlanda and S. Savasta, *Solid State Commun.* **91**, 157 (1994).
- ²⁷D. Fröhlich, A. Nöthe, and K. Reimann, *Phys. Rev. Lett.* **55**, 1335 (1985).